Enantioselective Oxidation of Racemic Phosphines with Chiral Oxoruthenium Porphyrins and Crystal Structure of [5,10,15,20-Tetrakis[*o*-((2-methoxy-2-phenyl-3,3,3-trifluoropropanoyl)amino)phenyl]porphyrinato](carbonyl)(tetrahydrofuran)ruthenium(II) ($\alpha,\beta,\alpha,\beta$ Isomer)†

Paul Le Maux, Hassan Bahri, and Gérard Simonneaux*

Laboratoire de Chimie Organométallique et Biologique, UA CNRS 415, Université de Rennes 1, Campus de Beaulieu, 35042 Rennes Cedex, France

Loic Toupet

Groupe Matière Condensée et Matériaux, UA CNRS 804, Université de Rennes 1, Campus de Beaulieu, 35042 Rennes Cedex, France

Received February 17, 1995⊗

The synthesis of dioxoruthenium(VI) picket-fence complexes bearing optically active α-methoxy-α-(trifluoromethyl)phenylacetyl residues on both sides of the porphyrin plane ($\alpha,\beta,\alpha,\beta$ and $\alpha,\alpha,\beta,\beta$ isomers) are described. These chiral porphyrins have been characterized by UV−visible, IR, and ^1H,^{13}C, and ^{19}F NMR spectroscopy. For benzylmethylphenylphosphine a chiral recognition was observed for the oxygen-atom transfer to phosphorus yielding optically active phosphine oxide with 41% enantiomeric excess. A mechanism for phosphine oxidation involving kinetic resolution to give an oxoruthenium(IV) intermediate is proposed. An X-ray crystal structure determination of the Ru(CO) complex of the $\alpha,\beta,\alpha,\beta$ isomer was carried out. Crystal data for $RuF_{12}O_{10}N_8C_{89}H_{64}$: $M_r = 1734.6$, orthorhombic, $P2_12_12_1$, a = 14.481(3) Å, $b = 22.729(6)$ Å, $c = 25.491(6)$ Å, $V = 8390(3)$ Å^{-3}, $Z = 4$, $D_X = 1.37$ Mg m^{-3}, λ (Mo K_α) = 0.709 26 Å, $\mu = 2.68$ cm^{-1}, $F(000) = 3544$, $T =$ 293 K, final $R = 0.070$ for 4198 observations.

Introduction

The transfer of oxene from metal−oxo species is a subject of fundamental significance because of its relevance to the biological activation of oxygen by hemoproteins such as P-450 enzymes.[1] Despite the importance of these proteins, mechanistic understanding of most processes is limited, both because of the complexity of the reactions[2] and because of a lack of well-understood model systems. The periodic relationship of ruthenium to iron has received recent attention in porphyrin chemistry.[3−5] The isolation and characterization of the first *trans*-dioxoruthenium(VI) porphyrin complex was recently reported by Groves and Quinn.[3a] One of the features of ruthenium porphyrins as catalysts is that, among a family of oxoruthenium complexes which are relatively stable, dioxo(tetramesitylporphyrinato)ruthenium(VI) catalyzes the aerobic epoxidation of olefins at ambient temperature and pressure.[3b]

We have been interested in the development of new chiral metalloporphyrins for regioselective and enantioselective oxidation of organic substrates. The control of coordination features that are part of these stereochemical studies is apparently very important. It appears that ruthenium must be able to stabilize intermediates for effective chiral recognition to occur. On the basis of these findings, we recently reported the synthesis of chiral ruthenium(II) porphyrins.[6] The regiochemistry of axial ligation after ruthenium insertion and the molecular recognition of racemic phosphines by chiral ruthenium(II) porphyrins were also described. In a previous communication, we briefly reported the preparation of the first optically active dioxoruthenium(VI) porphyrin complexes.[7] The present paper deals with the details in the (porphinato)dioxoruthenium addition to racemic phosphines and the reaction mechanism involving possible ruthenium(IV) porphyrins as intermediates.[3c] Along with the stereochemical study of this reaction, we also report the complementary results of an X-ray study structure determination of the ruthenium carbonyl porphyrin complex bearing the same chiral picket-fence residues. This structure is, to our knowledge, the first crystal structure of an optically active ruthenium porphyrin complex.[8]

† Dedicated to Professor René Dabard on the occasion of his 64th birthday.

⊗ Abstract published in *Advance ACS Abstracts,* August 1, 1995.

(1) (a) Guengerich, F. P.; MacDonald, T. L. *Acc. Chem. Res.* **1984**, *17*, 9. (b) Ortiz de Montellano, P. R., Ed. *Cytochromes P-450; Reactions, Mechanism, and Biochemistry*; Plenum: New York, 1986. (c) Collman, J. P.; Zhang, X.; Lee, V. J.; Uffelman, E. S.; Brauman, J. I. *Science* **1993**, *261*, 1404.

(2) Gopinath, E.; Bruice, T. C. *J. Am. Chem. Soc.* **1991**, *113*, 4657 and references therein.

(3) (a) Groves, J. T.; Quinn, R. *Inorg. Chem.* **1984**, *23*, 3844. (b) Groves, J. T. ; Quinn, R. *J. Am. Chem. Soc.* **1985**, *107*, 5790. (c) Groves J. T.; Ahn, K. H. *Inorg. Chem.* **1987**, *26*, 3831.

(4) (a) Leung, W. H.; Che, C. H. *J. Am. Chem. Soc.* **1989**, *111*, 8812. (b) Ho, C.; Leung, W. H.; Che, C. M. *J. Chem. Soc., Dalton Trans.* **1991**, 2933. (c) Huang, J. S.; Che, C. H.; Poon, C. K. *J. Chem. Soc., Chem. Commun.* **1992**, 161.

(5) Tokita, Y.; Yamaguchi, K.; Watanabe, Y.; Morishima, I. *Inorg. Chem.* **1993**, *32*, 329.

(6) (a) Le Maux, P.; Bahri, H.; Simonneaux, G. *J. Chem. Soc., Chem. Commun.* **1991**, 1350. (b) Le Maux, P.; Bahri, H.; Simonneaux, G. *Tetrahedron* **1993**, *49*, 1401.

(7) Le Maux, P.; Bahri, H.; Simonneaux, G. *J. Chem. Soc., Chem. Commun.* **1994**, 1287.

(8) The structure of a chiral porphyrin nickel complex has been recently determined. However two atropoisomers are present in the crystal lattice; see: Veyrat, M.; Maury, O.; Faverjon, F.; Over, D. E.; Ramasseul, R.; Marchon, J. C.; Turowska-Tyrk, I.; Scheidt, W. R. *Angew. Chem., Int. Ed. Engl.* **1994**, *33*, 220.

0020-1669/95/1334-4691$09.00/0

Experimental Section

Materials. $Ru_3(CO)_{12}$ was prepared from $RuCl_3$ and CO as previously reported.[9] *m*-CPBA (m-chloroperbenzoic acid; Janssen Chimica, 75%) was used as received. The solvents were distilled under argon before use. We previously reported the syntheses of optically active $\alpha\beta\alpha\beta$−Ru(L)(CO) and $\alpha\alpha\beta\beta$-Ru(L)(CO) isomers (L = 5,10,-15,20-tetrakis[*o*-((2-methoxy-2-phenyl-3,3,3,-trifluoropropanoyl)amino)-phenyl]porphyrin).[6]

Physical Measurements. UV−visible spectra were recorded on an Uvikon 941 spectrophotometer in dichloromethane. Infrared spectra were obtained in KBr on a Nicolet 205 FT-IR spectrophotometer. NMR spectra were recorded on a Bruker AC 300P spectrometer at 300 MHz (^1H, $CDCl_3$), at 75 MHz (^{13}C, $CDCl_3$), and at 280 MHz (^{19}F, $CDCl_3$). The COSY spectra (C−H) were recorded in the phase sensitive mode using the standard sequence.[10] Elemental analyses were performed by the Service Central d'Analyses (CNRS) at Vernaison, France.

Syntheses. $\alpha\beta\alpha\beta$-$Ru^{VI}L(O)_2$ (2a). The $\alpha\beta\alpha\beta$ isomer Ru(L)(CO)-(THF) (**1a**) (100 mg, 0.057 mmmol) was dissolved in toluene (2 mL), and then 2.2 equiv of *m*-CPBA was added to the solution. The resulting mixture was stirred for 5 min. Complex **2a** was isolated by addition of hexane. The red-purple solid was filtered out and washed with hexane (yield 80%). The completion of the reaction was indicated by the disappearance of "CO complex" at 1950 cm^{-1}. UV−vis (CH_2Cl_2) (λ_{max}/nm): 422 (ϵ 100 dm^3 $mmol^{-1}$ cm^{-1}), 516 (ϵ 12). IR (KBr) (ν/cm^{-1}): 823 (O=Ru=O). NMR data (δ/ppm) are as follows. ^{19}F: −69.53 (s, $4CF_3$). C: Phe(meso) C_1, 131.1; C_2(N), 134.4; C_3, 121.7; C_4, 130.7; C_5, 124. 2; C_6, 138.0. Porphyrin: C_{meso}, 117.3; C^{α}_{pyr}, 142.2, 142.4; C^{β}_{pyr}, 132.0, 132.3. Picket: C(CO) 164.0; C(CF_3 and C*), 83.2 and 83.5; C(OMe), 52.7; Phe C_o, 127.0; C_m, 128.2; C_p, 129.2. Anal. Found: C, 60.16; H, 3.75; N, 6.33; F, 13.02. Calcd for $C_{84}H_{60}N_8O_{10}F_{12}$-Ru: C, 60.39; H, 3.59; N, 6.71; F, 13.66.

$\alpha\alpha\beta\beta$-$Ru^{VI}L(O)_2$ (2b). The $\alpha\alpha\beta\beta$ isomer Ru(L)(CO)(THF) (**1b**) (100 mg, 0.057 mmol) was dissolved in toluene (2 mL), and then 2.2 equiv of *m*-CPBA was added to the solution. The resulting mixture was stirred for 5 min. Complex **2b** was isolated by addition of hexane. The red-purple solid was filtered out and washed with hexane (yield 80%). The completion of the reaction was indicated by the disappearance of "CO complex" at 1950 cm^{-1}. UV−vis (CH_2Cl_2) (λ_{max}/nm): 422 and 514. NMR data (δ/ppm) are as follows. ^{19}F: −69.62, −69.72 (2s, $4CF_3$). Anal. Found: C, 60.16; H, 3.75; N, 6.33; F, 13.02. Calcd for $C_{84}H_{60}N_8O_{10}F_{12}Ru$: C, 60.34; H, 3.60; N, 6.51; F, 13.49.

$\alpha\alpha\beta\beta$-$Ru^{II}L(CH_3CN)_2$ (3a). The $\alpha\beta\alpha\beta$ isomer Ru(L)(CO)(THF) (**1a**) (40 mg, 0.023 mmol) was dissolved in CH_3CN (200 mL), and then the solution was irradiated with UV lamp for 16 h. This method is similar to that previously reported by James and Dolphin.[11] After removal of the solvent under vacuum, the resulting solid is dissolved again in 20 mL of CH_2Cl_2 and then precipited by addition of 100 mL of hexane (85% yield). The completion of the reaction was indicated by the disappearance of "CO complex" at 1950 cm^{-1}. UV−vis (CH_2-Cl_2) (λ_{max}/nm): 423 and 510. IR (KBr) (ν/cm^{-1}): 2100 (CN). NMR data (δ/ppm) are as follows. ^{19}F: −70.38 (s, $4CF_3$).

Stoichiometric Reaction of $[Ru^{VI}(L)(O)_2]$ with Phosphines. Oxidation of phosphines with dioxoruthenium porphyrin complexes was directly followed by NMR. Reactions were generally run for 1 h with 15 mg (9×10^{-3} mmol) of **2** in $CDCl_3$ in NMR tubes under argon. Oxidation of 4 equiv of racemic benzylmethylphenylphosphine, added to the solution with a syringe, yielded 2 equiv of phosphine oxide and 2 equiv of metal-ligated phosphine. Similar oxidations were carried out with 6 and 10 equiv of racemic phosphines. Enantiomeric excesses (ee) of the phosphine oxides were determined using (*R*)-(−)-*N*-(3,5-dinitrobenzoyl)-α-phenylethylamine as a chiral shift reagent.[12] The *S*-configuration of the phosphine oxide[13] was determined by polarimetry, after removing the ruthenium complex by addition of hexane and filtration. The reagent was directly added to the NMR sample at the end of the reaction. The ee of the Ru-bound phosphine was determined by integration of CF_3 signals in ^{19}F NMR, from the mixture of the *RR*, *SS*, and *RS* diastereoisomers, as we previously reported.[6a]

X-ray Structure of the $\alpha\alpha\beta\beta$ Isomer of Ru(L)(CO)(THF). Crystals of the Ru^{II} derivative were grown by permitting a pentane−CH_2Cl_2 solution to evaporate slowly in air. A small amount of THF was added to the solution to complete the coordination sphere. No precautions were taken to exclude moisture. On the basis of the structure determination the resultant crystals are Ru(L)(CO)(THF).

Determination of the Crystal Structure of 1a. Data Collection. A crystal, ca. 0.25 × 0.25 × 0.35 mm, was placed on a CAD4 Enraf-Nonius automatic diffractometer with graphite-monochromatized Mo Kα radiation. All crystallographic data are given in Table 3. Cell parameters are obtained by fitting a set of 25 high-θ reflections. The data collection ($2\theta_{max} = 50°$, scan $\omega/2\theta = 1$, $t_{max} = 60$ s, $h = 0-17$, $k = 0-27$, $l = 0-30$ (*hkl* range), intensity controls without appreciable decay (0.2%)) gave 8079 reflections from which 4198 were independent with $I > 4\sigma(I)$.

Determination and Refinement of the Structure. After Lorentz and polarization corrections the structure was solved with direct methods which revealed the Ru and the N atoms. The remaining non-hydrogen atoms of the structure and a THF molecule coordinated with the Ru atom were found after successive scale factor and difference Fourrier calculations. After isotropic ($R = 0.10$) and then anisotropic refinement (0.08), some hydrogen atoms may be found with a difference Fourier, the remaining ones being set in theoretical positions. The whole structure was refined by full-matrix least-squares techniques (use of *F* magnitude; *x*, *y*, *z*, β_{ij} for Ru, O, N, and C atoms, *x*, *y*, *z* and B_{iso} for CF_3 and phenyl groups, and *x*, *y*, *z* fixed for H atoms; 842 variables and 4198 observations; $w = 1/\sigma(F_0)^2 = [\sigma^2(I) + (0.04F_o^2)^2]^{-1/2}$) with the resulting R = 0.075, $R_w = 0.070$, and $S_w = 0.43$ (residual $\varrho <$ 0.043 eA^{-3}). Atomic scattering factors were taken from ref 14. All the calculations were performed on a Digital Micro Vax 3100 computer with the MOLEN package (Enraf-Nonius, 1990).[15] It must be noticed that, due to a rather high thermal motion (but not a disorder) of the CF_3 and OCH_3 groups, the absolute configuration (already known) was not verified.

Results

Syntheses of Optically Active Dioxoruthenium(VI) Porphyrins. Groves and Quinn first reported the preparation of a monomeric dioxoruthenium(VI) porphyrin.[3a] The macrocycle was tetramesitylporphyrin, and the success was attributed to the steric hindrance imposed by the ortho methyl substituents. In connection with our studies on chiral recognition with metalloporphyrins it seemed interesting to investigate the preparation of dioxoruthenium porphyrins bearing optically active pickets. The steric hindrance imposed by these pickets may also prevents the dimerization. This method has been used successfully to stabilize dioxygen adducts of ruthenium(II) porphyrins.[16] Oxidation of $\alpha\beta\alpha\beta$-RuL(CO)(THF) (**1a**) was carried out by introducing *m*-CPBA in CH_2Cl_2 as previously reported by Groves.[3a] Thus a new species $\alpha\beta\alpha\beta$-$RuL(O)_2$ (**2a**) (Figure 1) with absorption at 422 and 516 nm was immediately formed. **2a** was obtained in high yield and is stable in the solid state for hours at room temperature. Very similar results were also obtained when the $\alpha\alpha\beta\beta$-RuL(CO)(THF) isomer **1b** was oxidized under the same conditions, yielding $\alpha\alpha\beta\beta$-$RuL(O)_2$ (**2b**). The success of the reaction with these two isomers is probably due to the presence of two chiral pickets on both sides

(9) Eady, C. R.; Jackson, P. F.; Johson, B. F. G.; Lewis, J.; Malatesta, M. C.; McPartlin, M.; Nelson W. J. H. *J. Chem. Soc., Dalton Trans.* **1980**, 383.
(10) (a) Marion, D.; Wuthrich, K. *Biochem. Biophys. Res. Commun.* **1983**, *113*, 967. (b) Rance, M.; Sorensen, O. W.; Bodenhausen, G.; Wagner, G.; Ernst, R. R.; Wuthrich, K. *Biochem. Biophys. Res. Commun.* **1983**, *117*, 479.
(11) Farrell, N.; Dolphin, D. H.; James, B. R. *J. Am. Chem. Soc.* **1978**, *100*, 324.
(12) Dunach, E.; Kagan, H. B. *Tetrahedron Lett.* **1985**, *26*, 2649.
(13) Kyba, E. P. *J. Am. Chem. Soc.* **1975**, *97*, 2554.
(14) *International Tables for X-ray Crystallography*; Kynoch: Birmingham, England, 1974; Vol. IV.
(15) (a) Frenz. B. A. *Enraf-Nonius Molecular Structure Determination Package*: MolEN Version 1990; Enraf-Nonius: Delft, The Netherlands. (b) Johnson, C. K. *ORTEP*; Report ORNL-3794; Oak Ridge National Laboratory: Oak Ridge, TN.
(16) Colman, J. P.; Brauman, J. I.; Fitzgerald, J. P.; Sparapany, J. W.; Ibers, J. A. *J. Am. Chem. Soc.* **1988**, *110*, 3486.

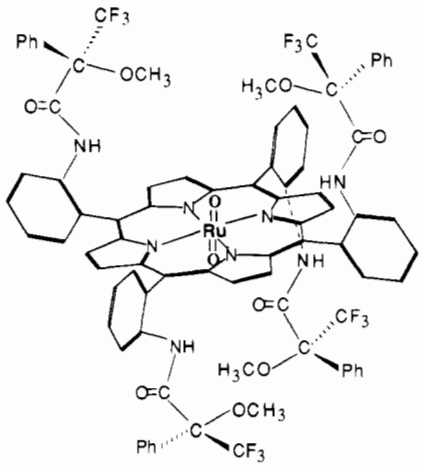

Figure 1. $[Ru^{VI}(O)_2(L)]$ (**2a**) ($\alpha\beta\alpha\beta$ isomer).

of the porphyrin plane.[4] The absence of hydrogen atoms on the pickets may also prevent any racemization.[17]

As expected for *trans*-dioxoruthenium, the oxidized products **2a** and **2b** afforded an IR absorption at 823 cm^{-1} indicative of O=Ru=O formation. This assignment is very similar to that of previously reported dioxoruthenium porphyrins.[3,4] The completion of the reaction is confirmed by the absence of the ν(CO) stretch at 1950 cm^{-1} in the IR spectrum.

NMR Spectroscopy of 1 and 2. The ^{1}H NMR data for **2a** and **2b** are listed in Table 1. For comparison, similar compounds, bearing the same chiral pickets and showing the same symmetry, are also summarized in Table 1. The ^{1}H NMR of both **2a** and **2b** are typical of diamagnetic compounds. Assignment of the signals was made from integration and comparison of their chemical shifts with those of the corresponding diamagnetic Ru(II) complexes. The symmetry properties of similar chiral porphyrins have been previously discussed.[6b] Thus compound **2a** shows D_2 symmetry and compound **2b** shows C_2 symmetry. Accordingly **2a** exhibited two singlets for the pyrrolic protons and **2b** exhibited three singlets for the pyrrolic protons. Interestingly, the methoxy unit is greatly shielded and appears at 0.73 ppm for **2a** and at 0.73 and 0.89 ppm for **2b** while the same group appears at 3.71 ppm in the chloride of α-methoxy-α-(trifluoromethyl)phenylacetic acid. As these signals were found 3 ppm upfield from the latter value, the methoxy protons must be located in the close vicinity of the porphyrin plane. A similar situation is found in the X-ray structure of the Ru(CO) complex (vide infra). Moreover, increasing the size of the ligand bound to the Ru atom leads to a deshielding effect and, for example, the methoxy group appears at 1.56 ppm for the $RuL[PMe_3]_2$ complex and 1.88 ppm for the $RuL[CH_3CN]_2$ complex (see Table 1). At this point the sharp and very-well defined peaks for each kind of protons in the ^{1}H NMR spectra of **2a** and **2b** agree with an absence of racemization.[18] However further NMR studies will be necessary in order to study the degree of freedom of these chiral pickets.

The ^{19}F spectra of **2a** and **2b**, showing one peak at −69.53 ppm and two peaks at −69.62 and −69.72 ppm, respectively, confirm the symmetry attributed to each atropisomer, D_2 and C_2, respectively.

Stoichiometric Oxidation of Racemic Phosphines by Dioxoruthenium(VI) Porphyrin. Since the formation of phosphine oxides from phosphines is indicative of chemically available oxo ligands in metal−oxo porphyrins,[3c] we first tested the addition of methyldiphenylphosphine to the chiral complex **2a**. As expected, addition of 4 equiv of the phosphine to dioxoruthenium porphyrin yielded 2 equiv of phosphine oxide and 2 equiv of $RuL[P(Me)(Ph)_2]_2$.[7]

In order to study the stereochemistry of oxygen atom transfer, benzylmethylphenylphosphine was chosen as a substrate since a quasi-complete chiral recognition was observed with this substrate during the complexation onto optically active complex **2a**.[6a] The percent of phosphine vs ruthenium complex concentration was varied from 4 to 10 in a series of different experiments. At the end of each experiment, the enantiomeric excess (ee) of the phosphine oxide was determined in situ, using *R*-(−)-*N*-(3,5-dinitrobenzoyl)-α-phenylethylamine as NMR resolving reagent, following the method previously reported by Kagan et al.[12] The methyl group which is seen as a doublet, due to the P−H coupling, is further separated in two peaks, when the chiral reagent is added to the solution. Integration of the signals gives directly the ee. Moreover the ee of the phosphine bound to ruthenium was also determined from the intensity of the CF_3 groups (^{19}F NMR) in the three diastereoisomers, as we previously reported.[6a] These results are summarized in Table 2. The reaction with 4 equiv of phosphine is described in eq 1.

$$\underset{\mathbf{2a}}{Ru(L)(O)_2} + 4PR_3 \rightarrow Ru(L)(PR_3)_2 + 2O{=}PR_3 \qquad (1)$$

Three important conclusions can be drawn from the data presented in Table 2: (i) Using an excess of phosphine, 2 equiv of phosphine oxide was obtained, corresponding to the oxygen atom transfer from Ru to the phosphorus atom. (ii) in each experiment, the phosphine oxide is optically active with the (−)-*S* configuration (the sign is obtained by polarimetry;[13] see Experimental Section). The ee is maximum when 4 equiv of phosphine is added to the solution. (iii) When **2a** was treated with 4 equiv of racemic phosphine, a 37.5:53.5:9 mixture of the three diastereoisomers (*SS*:*RS*::*RR*, respectively) was obtained. The preference per binding site was $S{:}R = 2.3$. In this reaction, the ee of the phosphine oxide is 41% ($S{:}R = 2.4$). The configurational correlation of oxidation of this phosphine is now well established, and oxidation with retention of (+)-(*R*)- benzylmethylphenylphosphine gave (−)-(*S*)-benzylmethylphenylphosphine oxide[13,19] (see Scheme 1). Accordingly, our data are consistent with oxidation with complete retention of configuration, within experimental error.

X-ray Structure of Ru(L)(CO)(THF). Suitable crystals for X-ray analysis were obtained by room-temperature evaporation of a CH_2Cl_2−pentane solution in air over 2 days. A small amount of THF was added to the solution to complete the coordination sphere. Crystal data and collection procedures are listed in Table 3. Selected atomic coordinates and *B* values (Å)^2 in crystalline **1a** are listed in Table 4. The molecular structure is shown in Figure 2. Key bond lengths and angles for the ruthenium complex are listed in Table 5. More complete bond distances and bond angles are listed in Tables 1S and 2S.[20]

The four equivalent Ru−N(pyrrole) distances average 2.046(9) Å which compares well with the distances of 2.049(5), 2.052(9), and 2.041(8) Å found for Ru(TPP)(CO)(EtOH),[21] Ru(TPP)(CO)(Pyr),[22] and $Ru(TPP)(Ph_2PCH_2PPh_2)_2$,[23] respectively (TPP for tetraphenylporphyrin).

The Ru−C(CO) distance of 1.79(1) Å seems reasonable. For example, the comparable distances are 1.77(2), 1.838(9), and

(17) Dale, J. A.; Mosher, H. S. *J. Am. Chem. Soc.* **1973**, *95*, 512.
(18) Renaud, J. P.; Battioni, P.; Mansuy, D. *New J. Chem.* **1987**, *11*, 279.
(19) Naumann, K.; Zon, G.; Mislow, K. *J. Am. Chem. Soc.* **1969**, *91*, 7012.
(20) Supporting information.
(21) Bonnet J. J.; Eaton, S. S.; Eaton, G. R.; Holm, R. H.; Ibers, J. A. *J. Am. Chem. Soc.* **1973**, *95*, 2141.
(22) Little, R. G.; Ibers, J. A. *J. Am. Chem. Soc.* **1973**, *95*, 8583.
(23) Ball, R. G.; Domazetis, G.; Dolphin, D.; James, B. R.; Trotter, *J. Inorg. Chem.* **1981**, *20*, 1556.

Table 1. ^{1}H NMR Data of Chiral Ruthenium Porphyrins with D_2 Symmetry ($\alpha\beta\alpha\beta$ Isomer) and C_2 Symmetry ($\alpha\alpha\beta\beta$ Isomer)

					H *meso* phenyl					
	OMe	NH amide	H phenyl picket	H_β pyrrole	H_3	H_4	H_5	H_6	NH pyrrole	ref
				$\alpha\beta\alpha\beta$ Isomer						
$Ru^{VI}(L)(O)_2$[a]	0.73, 1s	8.17, 1s	o-H, 6.60, d; m-H, 6.87, t; p-H, 7.11, t	8.97, 9.14, 2s	8.70, d	7.96, t	7.72, t	8.02, d		this work
$Ru^{II}(L)(PMe_3)_2$[b]	1.56, 1s	8.88, 1s	7.10−7.21, 1m	7.79, 8.04, 2s	8.86, d	7.72, t	7.36, t	7.35, d		6a
$Ru^{II}(L)(CH_3CN)_2$[c]	1.88, 1s	8.83, 1s	6.80−6.93, 1m	8.31, 8.19, 2s	9.33, d	7.50, t	7.19, t	7.80, d		this work
L	1.40, 1s	8.02, 1s	6.48, 1m	8.65, 8.83, 2s	8.56, d	7.90, t	7.65, t	8.07, d	−2.80, 1s	6b
				$\alpha\alpha\beta\beta$ Isomer						
$Ru^{VI}(L)(O)_2$	0.73, 0.89, 2s	8.27, 8.35, 2s	o-H, 6.66, 6.82, 2d; m-H, 6.97, 6.98, 2t; p-H, 7.12, 7.19, 2t	8.93, 9.12, 2s, 4H; 9.06, 1s, 4H	8.78, 8.82, 2dd	7.95, 7.98, 2td	7.68, 1tt	8.17, 8.20, 2dd		this work
$Ru^{II}(L)(PMe_3)_2$[d]	2.60, 2.86, 2s	8.97, 9.04, 2s	7.11−7.19, 1m	7.95, 8.15, 2s; 7.96, 8.04, 2d	8.81, 8.89, 2d	7.71, 7.72, 2t	7.35, 7.38, 2t	7.46, 7.52, 2d		6a
L	1.20, 1.54, 2s	8.15, 8.17, 2s	6.61−6.97, 1m	8.65, 8.80, 2s; 8.79, 8.32, 2d	8.68, 8.77, 2dd	7.89, 7.91, 2td	7.60, 7.61, 2td	7.98, 8.03, 2dd	−2.70, 1s	6b

[a] L = 5,10,15,20-tetrakis[*o*-((2-methoxy-2-phenyl-3,3,3-trifluoropropanoyl)amino)phenyl]porphyrin. [b] PMe_3, δ = −2.65 ppm (t). [c] CH_3CN, d = −0.66 ppm (s). [d] PMe3, d = −2.62 ppm (t).

Table 2. Data for the Oxidation of Racemic Benzylmethylphenylphosphine with **2a**

n[P(Me)(Ph)(CH_2Ph)] + **2a** → Ru(L)[P(Me)(Ph)(CH_2Ph)]$_2$ + 2[O=P(Me)(Ph)(CH_2Ph)] + (n − 4)[P(Me)(Ph)(CH_2Ph)]

[P(Me)(Ph)(CH_2Ph)] n, equiv	O=P(Me)(Ph)(CH_2Ph) (−)-*S* ee, %	complexed P(Me)(Ph)(CH_2Ph) (−)-*S* ee, %
4	41	40
6	25	34.5
10	12	47.3

Scheme 1. Oxidation of Benzylmethylphenylphosphine by [RuVI(L)$(O)_2$]

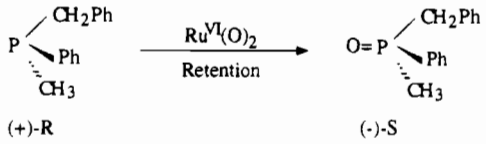

(+)-R (-)-S

Table 3. Crystallographic Data for **1a**

chem formula	$RuF_{12}O_{10}N_8C_{89}H_{64}$	Z	4
fw	1734.60	T, °C	24
space group	$P2_12_12_1$	λ, Å	0.709 26
a,[a] Å	14.481(3)	ϱ_{calc}, g·cm^{-3}	1.37
b,[a] Å	22.729(6)	μ(Mo Kα), cm^{-1}	2.68
c,[a] Å	25.491(6)	R[b]	0.075
V, Å^3	8390(3)	R_w[c]	0.070

[a] From a least-squares fitting of the setting angles of 25 reflections. [b] $R = \sum|F_o - F_c|/\sum F_o$. [c] $R_w = [\sum_w|F_o - F_c|^2/\sum_w F_o^2]^{1/2}$, with $w = 1/\sigma(F_o)^2 = [\sigma^2(I) + (0.04F_o^2)^2]^{-1/2}$.

1.811(5) Å in Ru(TPP)(CO)(EtOH),[21] Ru(TPP)(CO)(Pyr),[22] and Ru(TDCPP)(CO)(styrene oxide),[24] respectively (TDCPP for tetrakis(2,6-dichlorophenyl)porphyrin).

The axial Ru−O(THF) bond distance is 2.28(1) Å. This bond length may be compared with the Ru−O(THF) distance of 2.123(9) Å found in the complex Ru(TMP)(N_2)(THF)[25] (TMP for tetra-mesitylporphyrin). In light of this, the Ru−O(THF) distance observed in the Ru(CO)(THF) isomer is really quite long and may be related to a steric effect beween the chiral picket and the axial ligand or a different trans effect between CO and N_2. However, the Ru−O(THF) bond length may appear rather large in regard to the trans effect. The fact that the thermal motion of the THF molecule is rather important must also be considered. No definitive explanation can be given for this observation. However, this result is consistent with the kinetic lability of the THF ligand as observed by Groves et al.[26]

The C−O distance of 1.13(2) Å is normal as is the nearly linear angle for the two axial ligands, O−Ru−C = 179.0(5)°. As expected, the Ru−C−O group is essentially linear with an observed angle of 177(1)°. In contrast to the carbonyl heme proteins,[27] the Ru−C−O vector is within 1° of being perpendicular to the porphyrin plane.

The ruthenium atom is displaced 0.072(1) Å from the porphyrin plane toward the carbonyl ligand.

In common with other picket-fence porphyrin structures,[28] atoms of the chiral pickets are affected with high thermal motion but without disorder. However, the coordination sphere is reasonably precisely defined. Inspection of Figure 2 shows that OMe is located above the porphyrin plane. Such a situation was previously suggested from the high-field position of the methoxy group in the ^{1}H NMR spectrum.

Discussion

The study of the mechanism of oxygen atom transfer from an oxo metalloporphyrin complex to a substrate is a challenging problem which is of current interest in our understanding of heme-containing oxygenase selectivity. Various metalloporphyrins have been investigated as models in the catalytic insertion of oxygen into organic substrates.[29] Chiral metalloporphyrins especially have been used for asymmetric monooxygenations with good sucess.[30] In order to obtain additional

(24) Groves, J. T.; Han, Y.; Van Engen, D. *J. Chem. Soc., Chem. Commun.* **1990**, 436.
(25) Camenzind, M. J.; James, B. R.; Dolphin, D.; Sparapany, J. W.; Ibers, J. A. *Inorg. Chem.* **1988**, *27*, 3054.
(26) Groves, J. T.; Ahn, K. H.; Quinn, R. *J. Am. Chem. Soc.* **1988**, *110*, 4217.
(27) For a disccussion of the orientation of the Fe−CO group in hemoproteins, see for examples: Scheidt, W. R.; Haller, K. J.; Fons, M.; Mashiko, T.; Reed, C. A. *Biochemistry* **1981**, *20*, 3653. Baldwin, J. M. *J. Mol. Biol.* **1980**, *136*, 103.
(28) See for example: Jameson, G. B.; Molinaro, F. S.; Ibers, J. A.; Collman, J. P.; Brauman, J. I.; Rose, E.; Suslick, K. S. *J. Am. Chem. Soc.* **1980**, *102*, 3224 and references therein.
(29) For recent reviews, see for examples: Meunier, B. *Chem. Rev.* **1992**, *92*, 1411 and ref 1c.
(30) (a) Groves, J. T.; Myers, R. S. *J. Am. Chem. Soc.* **1983**, *105*, 5791. (b) Groves, J. T.; Viski, P. *J. Org. Chem.* **1990**, *55*, 3628. (c) O'Malley, S.; Kodadeck, T. *J. Am. Chem. Soc.* **1989**, *111*, 1916.

Table 4. Positional Parameters and Their Estimated Standard Deviations[a]

atom	*x*	*y*	*z*	*B*, Å^2	atom	*x*	*y*	*z*	*B*, Å^2
Ru	0.82639(8)	0.04318(5)	0.07911(4)	3.64(2)	C58	0.6031(9)	0.0184(6)	0.2226(5)	3.5(3)
F1	1.208(1)	−0.1579(6)	−0.1021(5)	12.1(4)*	C59	0.580(1)	0.0710(6)	0.2470(6)	5.2(4)
F2	1.223(1)	−0.1902(6)	−0.0242(5)	11.1(4)*	C60	0.515(1)	0.0750(7)	0.2832(6)	5.4(4)
F3	1.3219(9)	−0.1307(5)	−0.0559(4)	9.7(3)*	C61	0.468(1)	0.0258(7)	0.2994(6)	5.3(4)
F4	0.446(2)	0.2127(9)	−0.0911(9)	8.6(6)*	C62	0.488(1)	−0.0263(7)	0.2775(5)	5.2(4)
F5	0.431(1)	0.2686(8)	−0.0319(7)	6.5(4)*	C63	0.5561(9)	−0.0320(6)	0.2386(5)	4.2(3)
F6	0.334(1)	0.2059(8)	−0.0573(7)	6.8(4)*	C64	0.531(1)	−0.1359(8)	0.2144(8)	7.6(5)
F7	0.470(1)	−0.2621(7)	0.1989(7)	14.2(5)*	C65	0.579(1)	−0.1870(7)	0.1845(7)	6.1(4)
F8	0.570(1)	−0.2461(6)	0.2616(6)	11.8(4)*	C66	0.546(1)	−0.1880(8)	0.1299(7)	7.2(5)*
F9	0.611(1)	−0.2883(6)	0.1919(6)	11.7(4)*	C67	0.461(2)	−0.176(1)	0.115(1)	11.0(7)*
F10	0.839(1)	0.2612(6)	0.3563(5)	11.5(4)*	C68	0.437(3)	−0.175(2)	0.065(2)	19(1)*
F11	0.716(1)	0.2338(7)	0.3130(6)	13.9(5)*	C69	0.491(2)	−0.184(1)	0.025(1)	11.2(7)*
F12	0.823(1)	0.1675(6)	0.3295(5)	12.6(4)*	C70	0.612(2)	−0.195(1)	0.089(1)	11.4(7)*
O1	0.7583(9)	0.1639(5)	0.0736(5)	8.0(3)	C71	0.582(2)	−0.195(1)	0.035(1)	12.3(8)*
O2	0.8758(6)	−0.0520(5)	0.0842(4)	6.0(2)	C72	0.554(2)	−0.248(1)	0.2133(9)	10.2(7)*
O3	1.2301(7)	−0.0379(6)	−0.1110(4)	6.6(3)	C73	0.721(2)	−0.189(1)	0.231(1)	14(1)*
O4	1.0844(9)	−0.1060(6)	−0.0232(5)	9.2(3)	C74	1.0718(9)	0.0893(7)	0.2075(5)	4.6(3)
O5	0.3672(8)	0.0910(6)	−0.0381(6)	8.8(4)	C75	1.151(1)	0.0531(7)	0.2074(5)	4.9(4)
O6	0.5594(9)	0.1792(5)	−0.0170(5)	8.0(3)	C76	1.223(1)	0.0644(8)	0.2385(6)	5.8(4)
O7	0.454(1)	−0.1402(7)	0.2310(7)	13.9(4)	C77	1.221(1)	0.1110(8)	0.2732(6)	5.8(4)
O8	0.674(1)	−0.1806(6)	0.1840(5)	8.0(3)	C78	1.144(1)	0.1479(7)	0.2734(5)	5.1(4)
O9	1.010(1)	0.2309(6)	0.3107(5)	9.7(4)	C79	1.069(1)	0.1376(6)	0.2405(5)	4.1(3)
O10	0.825(1)	0.2024(5)	0.2270(6)	9.7(4)	C80	0.964(1)	0.2140(8)	0.2742(7)	6.9(5)
N1	0.9603(7)	0.0688(5)	0.0738(4)	4.1(2)	C81	0.865(1)	0.2371(8)	0.2640(6)	7.0(5)
N2	0.8223(8)	0.0356(5)	−0.0008(4)	4.4(2)	C82	0.865(1)	0.2997(8)	0.2529(8)	7.4(5)*
N3	0.6935(6)	0.0118(4)	0.0845(4)	3.7(2)	C83	0.932(2)	0.321(1)	0.226(1)	12.8(9)*
N4	0.8352(7)	0.0444(5)	0.1594(4)	3.9(2)	C84	0.934(2)	0.387(1)	0.208(1)	14.0(9)*
N5	1.1225(9)	0.0052(6)	−0.0585(5)	5.4(3)	C85	0.873(2)	0.415(1)	0.222(1)	12.1(8)*
N6	0.5214(8)	0.0762(5)	−0.0442(5)	5.1(3)	C86	0.804(2)	0.402(1)	0.243(1)	11.3(7)*
N7	0.5825(9)	−0.0865(5)	0.2166(5)	4.8(3)	C87	0.797(2)	0.341(1)	0.2627(9)	10.2(7)*
N8	0.9879(9)	0.1708(5)	0.2406(5)	5.2(3)	C88	0.813(2)	0.229(1)	0.319(1)	10.9(7)*
C1	1.0168(9)	0.0834(6)	0.1162(5)	3.9(3)	C89	0.757(2)	0.221(1)	0.195(1)	10.7(7)*
C2	1.103(1)	0.1044(7)	0.0959(5)	4.9(4)	H2	1.1564	0.1177	0.1168	5.0*
C3	1.098(1)	0.1037(8)	0.0434(6)	5.8(4)	H3	1.1445	0.1176	0.0186	5.0*
C4	1.0096(9)	0.0808(6)	0.0294(5)	4.2(3)	H7	0.8962	0.0409	−0.1179	5.0*
C5	0.973(1)	0.0749(7)	−0.0212(5)	4.9(4)	H8	0.7320	0.0078	−0.1159	5.0*
C6	0.8910(9)	0.0510(7)	−0.0344(5)	4.3(3)	H12	0.4953	−0.0289	0.0405	5.0*
C7	0.8594(9)	0.0374(9)	−0.0869(5)	6.1(4)	H13	0.4997	−0.0183	0.1385	5.0*
C8	0.773(1)	0.0179(7)	−0.0856(6)	5.4(4)	H17	0.7650	0.0295	0.2786	5.0*
C9	0.748(1)	0.0148(6)	−0.0307(5)	3.7(3)	H18	0.9296	0.0507	0.2720	5.0*
C10	0.6624(9)	−0.0033(6)	−0.0107(5)	3.8(3)	H27	0.9665	0.1743	−0.0755	5.0*
C11	0.6373(9)	−0.0021(6)	0.0419(5)	3.6(3)	H28	1.0676	0.2061	−0.1446	5.0*
C12	0.5474(9)	−0.0168(7)	0.0611(5)	4.5(3)	H29	1.1915	0.1511	−0.1715	5.0*
C13	0.551(1)	−0.0111(7)	0.1141(6)	4.8(4)	H30	1.2221	0.0609	−0.1316	5.0*
C14	0.6434(8)	0.0084(6)	0.1291(5)	3.9(3)	H35	1.2909	−0.0029	−0.0076	5.0*
C15	0.674(1)	0.0188(5)	0.1792(4)	3.5(3)	H36	1.3566	0.0201	0.0743	5.0*
C16	0.7639(9)	0.0320(6)	0.1932(5)	3.9(3)	H37	1.3055	−0.0252	0.1484	5.0*
C17	0.8006(9)	0.0345(7)	0.2469(5)	4.6(3)	H38	1.2120	−0.1105	0.1436	5.0*
C18	0.8875(9)	0.0481(7)	0.2429(5)	4.6(3)	H39	1.1458	−0.1363	0.0577	5.0*
C19	0.9124(9)	0.0568(6)	0.1885(5)	3.7(3)	H41A	0.9611	−0.1290	−0.0540	5.0*
C20	0.9959(9)	0.0749(6)	0.1693(5)	3.6(3)	H41B	1.0143	−0.0841	−0.0885	5.0*
C21	0.7856(9)	0.1175(6)	0.0747(6)	4.7(3)	H41C	1.0440	−0.1497	−0.0878	5.0*
C22	0.180(3)	0.398(2)	0.442(2)	7(1)*	H43	0.6450	−0.1019	−0.0622	5.0*
C23	0.888(3)	−0.154(2)	0.064(2)	5.6(9)*	H44	0.5227	−0.1353	−0.1184	5.0*
C24	0.942(6)	−0.137(4)	0.113(3)	6(2)*	H45	0.4113	−0.0686	−0.1449	5.0*
C25	0.952(3)	−0.074(2)	0.116(2)	6(1)*	H46	0.4045	0.0274	−0.1108	5.0*
C26	1.038(1)	0.0931(6)	−0.0659(5)	4.6(3)	H51	0.5535	0.1333	0.0720	5.0*
C27	1.021(1)	0.1491(8)	−0.0892(7)	6.9(5)	H52	0.4896	0.1201	0.1618	5.0*
C28	1.080(2)	0.1681(9)	−0.1275(7)	8.7(6)	H53	0.3599	0.1442	0.1754	5.0*
C29	1.152(1)	0.1361(8)	−0.1438(6)	6.5(4)	H54	0.2709	0.2151	0.1407	5.0*
C30	1.166(1)	0.0846(7)	−0.1211(6)	5.8(4)	H55	0.3107	0.2305	0.0357	5.0*
C31	1.1093(8)	0.0613(6)	−0.0831(5)	4.2(3)	H57A	0.6706	0.2331	0.0003	5.0*
C32	1.181(1)	−0.0369(7)	−0.0728(5)	5.1(3)	H57B	0.5808	0.2688	−0.0090	5.0*
C33	1.173(1)	−0.0888(8)	−0.0333(6)	6.6(4)	H57C	0.5954	0.2358	0.0436	5.0*
C34	1.215(1)	−0.0706(7)	0.0185(6)	5.9(4)*	H59	0.6119	0.1075	0.2352	5.0*
C35	1.273(1)	−0.0255(7)	0.0238(7)	6.2(4)*	H60	0.4992	0.1134	0.2980	5.0*
C36	1.310(1)	−0.0107(8)	0.0713(8)	7.7(5)*	H61	0.4194	0.0293	0.3251	5.0*
C37	1.284(1)	−0.040(1)	0.1142(8)	8.5(5)*	H62	0.4555	−0.0621	0.2895	5.0*
C38	1.226(2)	−0.089(1)	0.1104(9)	10.3(7)*	H67	0.4141	−0.1713	0.1446	5.0*
C39	1.187(2)	−0.1021(9)	0.0624(8)	8.9(5)*	H68	0.3682	−0.1645	0.0601	5.0*
C40	1.242(2)	−0.1440(9)	−0.0561(8)	8.6(6)*	H69	0.4691	−0.1783	−0.0112	5.0*
C41	1.027(2)	−0.118(1)	−0.064(1)	13.9(9)*	H70	0.6801	−0.1992	0.0957	5.0*
C42	0.5907(9)	−0.0208(6)	−0.0488(5)	3.7(3)	H71	0.6232	−0.2027	0.0071	5.0*
C43	0.593(1)	−0.0750(6)	−0.0706(5)	4.6(3)	H73A	0.7896	−0.1841	0.2291	5.0*
C44	0.525(1)	−0.0947(8)	−0.1064(6)	5.7(4)	H73B	0.7042	−0.1627	0.2605	5.0*
C45	0.459(1)	−0.0569(8)	−0.1191(6)	6.5(4)	H73C	0.7153	−0.2289	0.2472	5.0*
C46	0.453(1)	−0.0001(7)	−0.0992(6)	5.5(4)	H75	1.1515	0.0181	0.1844	5.0*
C47	0.519(1)	0.0188(7)	−0.0648(5)	4.6(3)	H76	1.2793	0.0390	0.2376	5.0*
C48	0.447(1)	0.1063(7)	−0.0339(6)	5.6(4)	H77	1.2720	0.1184	0.2977	5.0*
C49	0.465(1)	0.1716(8)	−0.0118(8)	7.0(5)	H78	1.1429	0.1812	0.2977	5.0*
C50	0.430(1)	0.1708(9)	0.0474(7)	7.2(5)*	H83	0.9853	0.2965	0.2118	5.0*
C51	0.486(2)	0.148(1)	0.082(1)	14.1(9)*	H84	0.9932	0.4063	0.1900	5.0*
C52	0.449(2)	0.142(1)	0.136(1)	14(1)*	H85	0.8726	0.4585	0.2100	5.0*
C53	0.378(2)	0.165(1)	0.141(1)	12.8(8)*	H86	0.7502	0.4291	0.2499	5.0*
C54	0.322(3)	0.198(1)	0.117(1)	16(1)*	H87	0.7420	0.3282	0.2837	5.0*
C55	0.346(2)	0.204(1)	0.061(1)	13.4(9)*	H89A	0.7353	0.1899	0.1703	5.0*
C56	0.414(2)	0.215(1)	−0.053(1)	5.9(8)*	H89B	0.7009	0.2342	0.2122	5.0*
C57	0.604(2)	0.232(1)	0.006(1)	11.9(8)*	H89C	0.7748	0.2533	0.1715	5.0*

[a] Starred *B* values are for atoms that were refined isotropically. Anisotropically refined atoms are given in the form of the isotropic *equivalent* displacement parameter defined as $(4/3)[a^2B(1,1) + b^2B(2,2) + c^2B(3,3) + ab(\cos\gamma)B(1,2) + ac(\cos\beta)B(1,3) + bc(\cos\alpha)B(2,3)]$.

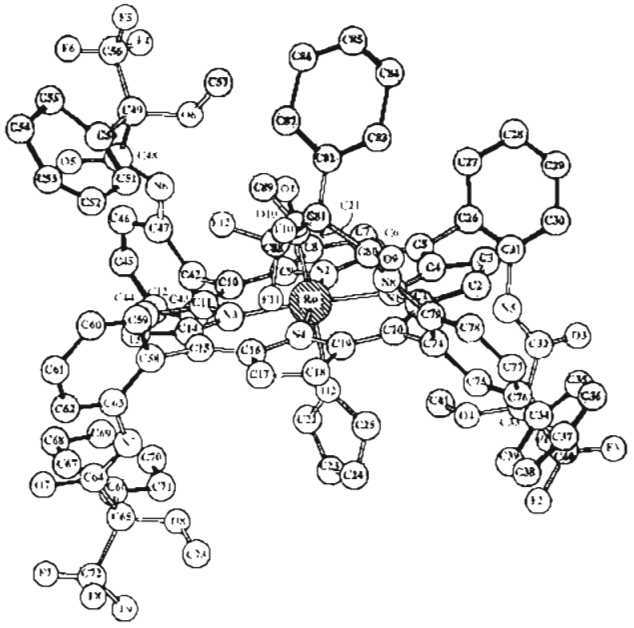

Figure 2. Molecular structure of Ru(L)(CO)(THF).

Table 5. Selected Bond Distances (Å) and Bond Angles (deg) for Ru(L)(CO)(THF)[a]

	Distances		
Ru−O2	2.28(1)	Ru−N4	2.052(9)
Ru−N1	2.03(1)	Ru−C21	1.79(1)
Ru−N2	2.045(9)	O1−C21	1.13(2)
Ru−N3	2.057(9)		
	Angles		
Ru−C21−O1	177(1)	N1−Ru−C21	92.3(5)
O2−Ru−N1	88.6(4)	N2−Ru−N3	90.6(4)
O2−Ru−N2	89.2(4)	N2−Ru−N4	175.5(5)
O2−Ru−N3	87.7(4)	N2−Ru−C21	90.4(6)
O2−Ru−N4	86.4(4)	N3−Ru−N4	89.8(4)
O2−Ru−C21	179.0(5)	N3−Ru−C21	91.3(5)
N1−Ru−N2	89.2(4)	N3−Ru−N4	89.8(4)
N1−Ru−N3	176.4(4)	N3−Ru−C21	91.3(5)
N1−Ru−N4	90.2(4)	N4−Ru−C21	94.0(6)

[a] Standard deviations in parentheses.

information on the stereochemistry of oxygen atom transfer from metal to substrate, it is important to design a chiral metalloporphyrin system so that the nature of the reactive species can be clarified unambiguously. To achieve chiral recognition, the chiral groups should also be inert to oxidation and to racemization. To design a metalloporphyrin which satisfies the requirement above, we utilized a porphyrin inert framework, using the Mosher reagent to provide chiral groups, and a ruthenium coordination site. Another advantage of using ruthenium porphyrins as chiral oxygen atom transfer systems is that these metalloporphyrins could be a model for the heme-containing monooxygenases due to the periodic relationship of ruthenium to iron.

We previously reported the molecular recognition of racemic phosphines by chiral ruthenium(II) porphyrins. Complexation of racemic benzylmethylphenylphosphine to the $\alpha\beta\alpha\beta$ isomer leads to the formation of one of three possible product diastereoisomers with high degree of selectivity (complexation of the (*S*)-phosphine). This result was obtained under kinetic control whereas thermodynamic control yielded less favorable recognition. In the present paper, we report the oxidation of the same phosphine to phosphine oxide by a chiral dioxoruthenium porphyrin. Surprisingly, this reaction gave the inverted selectivity since it is the (*R*) enantiomer which was preferably oxidized.

Scheme 2. Oxidation Mechanism of Chiral Phosphine (4 equiv)

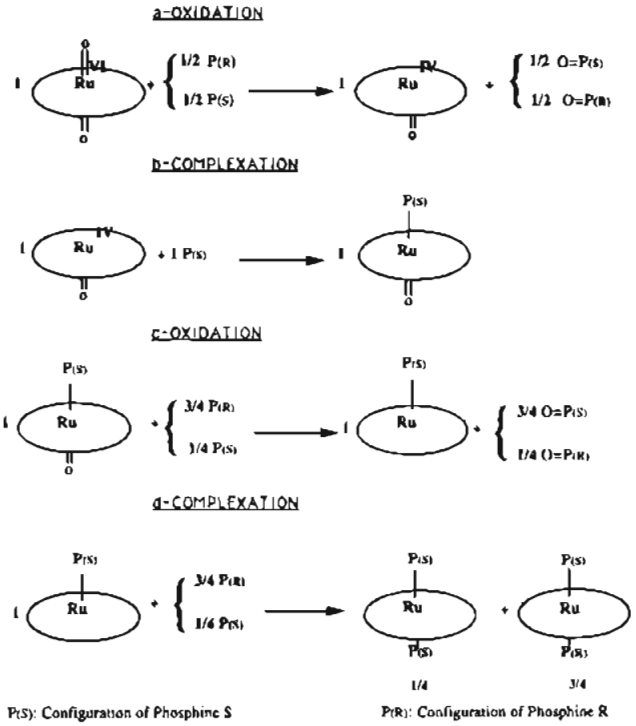

P(S): Configuration of Phosphine S P(R): Configuration of Phosphine R

In order to explain the inverted selectivity and the decrease of the selectivity with increasing amount of the phosphine (Table 2), we proposed the mechanism summarized in Scheme 2. The analysis is based on 4 equiv of phosphine. This mechanism is discussed with the first assumption of oxene transfer without chiral recognition. The reactivity of $Ru^{VI}(O)_2$ is such that it can attack either the *R* or *S* isomer of the phosphine to form $Ru^{IV}(O)$ (step a). Thus the initial product of the reaction contains racemic phosphine oxide. Unlike the first step, we propose a complete stereoselectivity in the complexation of chiral benzylmethylphenylphosphine to the $Ru^{IV}(O)$ intermediate. This will lead to one of the two possible diastereoisomers: $Ru^{IV}(O)(P_S)$ (step b). It is worth noting that such stereoselectivity was previously observed during the complexation of the phosphine onto Ru.[6a] The behavior of the $Ru^{IV}(O)$ complex, reported in step c, parallels that of its $Ru^{IV}(O)$ congeners,[3,31] which also are capable of oxygen-atom transfer to oxidize triphenylphosphine to triphenylphosphine oxide. However, the product formed in the second oxidation, i.e. phosphine oxide, is now optically active since the substrate, i.e. the phosphine, is also optically active . We also suppose in step c a transfer without chiral recognition. Finally complexation of the 2 equiv of the remaining phosphine will occur in step d. In this particular case, a simple calculation will give (*S*)-phosphine oxide with 25% ee. The experimental result gives (*S*)-phosphine oxide with 41% ee. This is evidence for an oxygen-atom transfer with chiral recognition under kinetic resolution. This interpretation is also in agreement with a decrease in selectivity when a large excess of phosphine is used (10 equiv). In this case, the contribution of chiral recognition in step b (the (*S*)-phosphine complexation to the $Ru^{IV}(O)$ intermediate) is very weak (ee: 6.25%). The experimental result gives (*S*)-phosphine oxide with 12% ee. A weak chiral recognition during the oxygen-atom transfer is also clearly operating here, even with addition of a large excess of the racemic phosphine. Attempts to isolate pure $Ru^{IV}(O)$ are at

(31) James, B. R.; Mikkelsen, S. R.; Leung, T. W.; Williams, G. M.; Wong, R. *Inorg. Chim. Acta* **1984**, *85*, 209.

present ineffective although four signals at −18.87, −24.08, −28.61, and −33.62 ppm were observed in the ^{1}H NMR spectra during a progressive addition of the phosphine to **2a**. A high-field chemical shift (−10 ppm) has been previously reported for Ru^{IV}(TMP)(O) for the pyrrole protons,[3c] and the multiplicity of these signals well agree with the expected C_2 symmetry. A fast reaction of this quite basic phosphine with Ru^{IV}(O) complex possibly explains why this intermediate is difficult to get as a pure compound. Further, the good correlation between the preference of the binding site to the ruthenium and the ee of the phosphine oxide implies an oxygen-atom transfer which proceeds with retention of phosphorus configuration.

Direct comparison of the selectivity observed between complexation and oxygen-atom transfer will need further studies. However, it is worth noting that the relative positions of the incoming substrate and the chiral pickets are very different in each case; in particular, the Ru−P distance is much longer for the oxygen-atom transfer than for the metal complexation. In the latter case, the ^{1}H NMR spectrum of the complex RuL[P(Me)(CH_2Ph)(Ph)]$_2$ [(*S*) enantiomer][6a] shows a methoxy group at 2.69 ppm whereas the chemical shift for the same group in **2a** is 0.73 ppm (Table 1). Thus, a large displacement of the chiral picket is expected after complexation of the phosphine, from the NMR results (δ = 2 ppm). Interestingly, both the X-ray structure and the NMR spectra suggest a possible interaction between the methoxy groups of the chiral pickets and bulky ligands (substrates). Further work will be directed toward determining if the methoxy group is exerting a partial gating for the incoming substrates.

Conclusion

In conclusion, novel optically active dioxoruthenium(VI) porphyrins were prepared in the stoichiometric oxidation of ruthenium(II) carbonyl porphyrins. Further, oxidation reactions of racemic phosphines were carried out, and a mechanism for the oxygen transfer is proposed. The results show both an absence of racemization and a chiral recognition during the oxygen-atom transfer. In comparison with the molecular recognition of racemic phosphines by chiral ruthenium(II) porphyrins, the oxidation reaction gave the inverted selectivity since it is the (*R*) enantiomer which was preferably oxidized. An X-ray crystal structure determination of the Ru(CO) complex of the $\alpha\beta\alpha\beta$ isomer was carried out, and the result shows the methoxy groups of the chiral pickets above the porphyrin plane.

Acknowledgment. We thank A. Bondon for performing 2D NMR spectra.

Supporting Information Available: Complete tables of bond distances and angles (7 pages). Ordering information is given on any current masthead page.

IC9501881